# Research

## Advanced Materials and Materials Genome——Review

# Research and Development of Heat-Resistant Materials for Advanced USC Power Plants with Steam Temperatures of 700 °C and Above

Fujio Abe

**ABSTRACT** Materials-development projects for advanced ultra-supercritical (A-USC) power plants with steam temperatures of 700 °C and above have been performed in order to achieve high efficiency and low $CO_2$ emissions in Europe, the US, Japan, and recently in China and India as well. These projects involve the replacement of martensitic 9%–12% Cr steels with nickel (Ni)-base alloys for the highest temperature boiler and turbine components in order to provide sufficient creep strength at 700 °C and above. To minimize the requirement for expensive Ni-base alloys, martensitic 9%–12% Cr steels can be applied to the next highest temperature components of an A-USC power plant, up to a maximum of 650 °C. This paper comprehensively describes the research and development of Ni-base alloys and martensitic 9%–12% Cr steels for thick section boiler and turbine components of A-USC power plants, mainly focusing on the long-term creep-rupture strength of base metal and welded joints, strength loss in welded joints, creep-fatigue properties, and microstructure evolution during exposure at elevated temperatures.

**KEYWORDS** Ni-base alloy, 9%–12% Cr steel, creep strength, creep-fatigue property, welded joint, grain boundary, microstructure, γ′, $M_{23}C_6$ carbide

## 1 Introduction

Energy security combined with lower carbon dioxide ($CO_2$) emissions is increasingly necessary to protect the global environment in the 21st century. Coal provides us with abundant, low-cost resources for electric power generation. However, traditional coal-fired power plants have been emitting environmentally damaging gases such as $CO_2$, $NO_x$, and $SO_x$ at high levels relative to other electric power generation options, such as nuclear power plants, combined-cycle gas turbines, and so on. The adoption of ultra-supercritical (USC) power plants with increased steam parameters significantly improves efficiency, which reduces fuel consumption and the emission of environmentally damaging gases. The present USC power plants with steam temperatures at around 600 °C utilize martensitic 9%–12% Cr steels for thick section components such as main steam pipes and headers in boilers and for turbine rotors and high-strength austenitic steels for superheat tubes [1]. Martensitic 9%–12% Cr steels such as ASME Gr. 91 (9Cr-1Mo-0.2V-0.05Nb), Gr. 92 (9Cr-0.5Mo-1.8W-VNb), and Gr. 122 (11Cr-0.4Mo-2W-1CuVNb) can offer the highest potential to meet the required flexibility for USC power plants, because of their smaller thermal expansion and larger thermal conductivity as compared with austenitic steels and nickel (Ni)-base alloys.

Materials-development projects for advanced ultra-supercritical (A-USC) power plants with steam temperatures of 700 °C and above have been performed in order to achieve high efficiency in Europe (the AD700 project initiated in 1998 [2], the COMTES700 project [3, 4], the GKM HWT II project [5], the ENCIO project [6], etc.), in the US (the US DOE/OCDO A-USC project initiated in 2001 [7–9]), in Japan (the A-USC project initiated in 2008 [10]), and recently in China (the National R&D Project of 700 °C USC Power Generation Technology in China initiated in 2011 [11, 12]) and in India (the National Mission for the Development of A-USC Technology initiated in 2012 [13]). The full names for the A-USC projects are as follows. AD700: Advanced Supercritical 700 °C Pulverized Coal-Fired Power Plant. COMTES700: Component Test Facility for 700 °C Power Plant. GKM HWT: Grosskraftwerk Mannheim Hochtemperatur Werkstoff Teststrecke. ENCIO: European Network for Component Integration and Optimization. US DOE/OCDO: the United States Department of Energy and Ohio Coal Development Office.

The US DOE/OCDO A-USC project aims at a steam tem-

National Institute for Materials Science, Tsukuba 305-0047, Japan
E-mail: ABE.Fujio@nims.go.jp

perature of 760 °C (1400 °F) and a pressure of 35 MPa, while the other projects in Europe, Japan, China, and India aim at a steam temperature of 700 °C. These projects all involve the replacement of martensitic 9%–12% Cr steels with Ni-base alloys for the highest temperature boiler and turbine components in order to ensure sufficient creep strength. It should be noted that Ni-base alloys are much more expensive than ferritic/martensitic steels. To minimize the requirement for expensive Ni-base alloys, martensitic 9%–12% Cr steels can be applied to the next highest temperature components of A-USC power plants. Therefore, it is very desirable for martensitic 9%–12% Cr steels to be developed that have an increased temperature range from their current maximum of 610–620 °C up to 650 °C.

This paper comprehensively describes the research and development of Ni-base alloys and martensitic 9%–12% Cr steels for thick section boiler and turbine components of A-USC power plants. Greater attention will be paid to technical issues regarding the use of Ni-base alloys in high-temperature thick section components of A-USC power plants.

## 2 Creep strength required for power-plant steels and alloys

High-temperature components such as the boilers of power plants are designed using allowable stress under creep conditions, which is usually determined on the basis of a 100 000 h creep-rupture strength at the operating temperature, and sometimes also 200 000 h to 500 000 h creep-rupture strength [14]. For instance, the 100 000 h creep-rupture strength is defined as the stress at which creep rupture occurs at 100 000 h. In an elevated-temperature creep region, for example, the allowable stress in ASME Section II (i.e., Section II of the Boiler and Pressure Vessel Code by the American Society of Mechanical Engineers (ASME)) is determined by several factors, such as 100% of the average stress to produce a creep rate of 0.01%/1000 h (= $10^{-5}$%·$h^{-1}$), 67% of the average stress (below 815 °C), and 80% of the minimum stress to cause rupture at the end of 100 000 h [15]. An evaluation of the stress required to produce a minimum creep rate of $10^{-5}$%·$h^{-1}$ and the stress required to cause rupture at the end of 100 000 h for a number of ferritic and austenitic steels and Ni-base and Co-base alloys using long-term creep and creep-rupture data in National Institute for Materials Science (NIMS) Creep Data Sheets showed that the ASME allowable stress was determined by the creep-rupture data but not by the creep-strain rate data [16]. Therefore, a deciding criterion for the creep resistance of power-plant steels and alloys is usually 100 000 h creep-rupture strength at the operating temperature. The target stress value for 100 000 h creep-rupture strength is usually 100 MPa for base metal at the operating temperature.

Critical issues for long-term safe operation of candidate Ni-base alloys and martensitic 9%–12% Cr steels for A-USC power plants include oxidation resistance in steam as well as the long-term creep-rupture strength of base metal and welded joints. Resistance to strength loss, such as Type IV cracking in welded joints, is a serious issue for welded thick section boilers as well as for welded turbine rotors. Furthermore, the thermal-cycling capabilities of thick section components in

A-USC power plants would be severely restricted by creep-fatigue damage. The discontinuous or flexible operation mode in A-USC power plants, including daily start-up in the morning and shut-down at night, needs to have good thermal flexibility for thick section components, namely, low thermal expansion, high thermal conductivity, and enough resistance to creep-fatigue damage.

Traditionally, the development of Ni-base alloys with higher creep strength than ferritic and austenitic steels has been achieved mainly for application to gas turbine components. Some gas turbine alloys are now candidates for the highest temperature components of boilers and turbines in A-USC power plants with maximum steam temperatures of 700 °C and above. The Ni-base alloys used for the main steam pipe in boilers and for turbine rotors are wrought materials, not cast ones. For wrought materials, not only sufficient creep strength but also excellent hot workability and weldability are required. The primary strengthening mechanism of conventional Ni-base alloys is precipitation hardening due to the $\gamma'$ phase of $Ni_3(Al, Ti)$.

Figure 1 shows the temperature dependence of the 100 000 h creep-rupture strength of conventional martensitic 9%–12% Cr steels, austenitic steels, and Ni-base alloys [8, 9]. Nominal compositions of some Ni-base alloys for A-USC power plants are given in Table 1 [9]. In Figure 1, some Ni-base alloys, such as Alloys 740, 282, 617, and 230, satisfy the 100 000 h creep-rupture strength of 100 MPa at 700 °C, while no martensitic 9%–12% Cr steel satisfies 100 MPa at 650 °C. The creep strength of Ni-base alloys is correlated with the amount of $\gamma'$ precipitates $Ni_3(Al, Ti)$ in the alloys. The larger the amount of $\gamma'$ is, the higher the creep strength is. Figure 2 shows the amount of $\gamma'$ precipitates, estimated by Toda at NIMS by using Thermo-Calc, in Alloy 740 and Alloy 617. The amount of $\gamma'$ is three times larger in Alloy 740 than in Alloy 617 at 700 °C, causing a much higher creep strength in Alloy 740 than in CCA 617, which is the variant of Alloy 617, as shown in Figure 1. Alloy 740 and Alloy 282 are strongly hardened by a large amount of fine $\gamma'$ precipitates, as can be expected by high aluminum and titanium content. On the other hand, hot working becomes difficult when increasing the amount of $\gamma'$ precipitates.
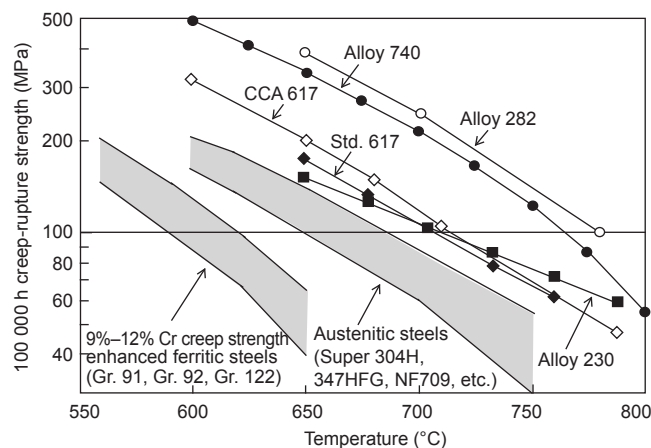


**Figure 1. 100 000 h creep-rupture strength of some Ni-base superalloys, together with 9%–12% Cr creep strength enhanced ferritic steels and austenitic steels, as a function of temperature.**

**Table 1. Nominal compositions of some Ni-base alloys for A-USC power plants (unit: %, mass fraction).**

| Alloy | C | Cr | Mo | Co | Al | Ti | Mn | Si | Ni | Others |
|---|---|---|---|---|---|---|---|---|---|---|
| **617** | 0.10* | 22 | 9.0 | 12 | 1.2 | 0.3 | 1.0* | 1.0* | Bal | Fe: 3.0*; B: 0.006* |
| **625** | 0.10* | 21 | 9.0 | 1* | 0.4* | 0.4* | 0.1* | 0.5* | Bal | Fe: 5; Nb: 3.7 |
| **740** | 0.03 | 25 | 0.5 | 20 | 0.9 | 1.8 | 0.3 | 0.5 | Bal | Fe: 0.7; Nb: 2.0 |
| **740H** | 0.03 | 25 | 0.5 | 20 | 1.35 | 1.35 | 0.3 | 0.15 | Bal | Fe: 0.7; Nb: 1.5 |
| **230** | 0.10 | 22 | 2.0 | 5* | 0.3 | — | 0.5 | 0.4 | Bal | W: 14; Fe: 3*; La: 0.02; B: 0.015* |
| **263** | 0.06 | 20 | 6.0 | 20 | 0.6* | 2.4* | 0.6* | 0.4* | Bal | Fe: 0.7*; Cu: 0.2* |
| **282** | 0.06 | 20 | 8.0 | 10 | 1.5 | 2.1 | 0.3* | 0.15* | Bal | Fe: 1.5*; B: 0.005 |
| **105** | 0.17* | 15 | 5.0 | 20 | 4.7 | 1.2 | 1.0* | 1.0* | Bal | Fe: 1.0*; B: 0.007 |
| **Waspalloy** | 0.02–0.10 | 18–21 | 3.5–5.0 | 12.0–15.0 | 1.2–1.6 | 2.75–3.50 | 0.1* | 0.1* | Bal | Fe: 2.0*; B: 0.003–0.010 |

**Note:** *maximum.
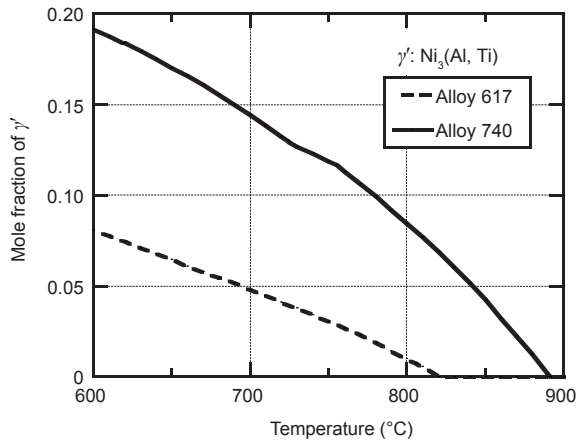


**Figure 2. Mole fraction of $\gamma'$ precipitates in Alloy 617 and Alloy 740 as a function of temperature.**

# 3 Ni-base alloys for highest temperature components of A-USC power plants

## 3.1 Candidate Ni-base alloys in the US

Table 2 summarizes key Ni-base alloys under evaluation in the US DOE/OCDO A-USC project, together with some comments on their applicability and limitations [9]. The intended maximum steam temperature in the US DOE/OCDO A-USC project is 760 °C, which is higher than in the other programs worldwide that are focused on A-USC at 700 °C. This desire for a higher maximum has led to the extensive study of Alloy 740 and Alloy 282. A variety of progress has been made in advancing the materials technology to enable 760 °C A-USC power plants, such as the demonstration of welding and fabrication of Ni-base alloys for A-USC plants; the evaluation of creep-rupture strength, notch sensitivity, microstructure stability, steam oxidation, and fireside corrosion resistance; the development of casting techniques for $\gamma'$-precipitation hardened Ni-base alloys with high Ti and Al content; and so on. The US DOE/OCDO A-USC project consortium has identified that Alloy 740/740H is suitable for main steam pipes, as well as for superheater (SH) and reheater (RH) tubes, for long-term service under A-USC conditions, while Alloy 282 is promising for turbine rotors and discs.

Alloy 740 is a $\gamma'$ (Ni$_3$Al)-precipitation hardened Ni-base alloy developed for use as SH and RH tubing in A-USC power plants. Due to its excellent creep-rupture strength and corrosion resistance, the consortium also evaluated its use for thick section components such as boiler piping and headers [9]. However, when Alloy 740 became a leading candidate for thick section components envisioned for service to 760 °C in the US DOE/OCDO A-USC project, it became evident that some adjustments to the original chemistry would be needed.

**Table 2. Ni-base alloys under evaluation in the US DOE/OCDO A-USC project.**

| Alloy | Component | Comments |
|---|---|---|
| **230** | SH/RH, pipe | Successful welding trials, maximum size limitations for pipe may limit applicability |
| **CCA 617** | SH/RH, pipe | Higher strength than 617 but not enough data to change ASME code stress values, not suitable for high sulfur coals, only successful SMAW welds in Ni-base alloys, strain-age cracking concerns, low strength limits applicability for turbine rotor |
| **263** | Castings, rotor | Back-up cast alloy to 282, good castability and weldability, lower strength but good ductility |
| **740/740H** | SH/RH, pipe | Highest strength alloy in *ASME B&PV Code* to enable A-USC up to 760 °C (1400 °F), excellent fireside corrosion resistance, successful fabrication and welding, prome candidate for boiler components, cannot be air cast for valves and shells |
| **282** | Castings, rotor | Higher creep strength than 740, relatively insensitive to starting microstructural condition, good forging "window" for rotor, can be cast for valves and casings |
| **Waspalloy** | Rotor, bolts, blades | Back-up alloy with good turbine history, cannot be welded reliability, poor ductility |
| **105** | Bolts, blades | Highest creep strength alloy, only considered for bolting and blading (non-welded components) |

**Notes:** SMAW—shielded metal arc welding; B&PV—boiler and pressure vessel.

The work done to evaluate the capability of the original composition in thick section weldments revealed a tendency for Alloy 740 to form micro-fissures or micro-cracks in the heat-affected zone (HAZ), although micro-fissures or micro-cracks in the HAZ have not been encountered in thin-walled tube welds. Attention was also paid to microstructure stability during exposure to 700–850 °C. Xie et al. and Zhao et al. performed an extensive metallographic analysis of Alloy 740, aging it for up to 5000 h at temperatures of 704–850 °C [17, 18]. Their work revealed that during exposure at 725 °C and above, acicular $\eta$-phase ($Ni_3Ti$) particles nucleated at grain boundaries and grew inside the grains while consuming $\gamma'$ precipitates. Specific adjustments in chemistry that were explored included: increasing the Al/Ti concentration ratio slightly to improve the stability of $\gamma'$ during exposure at elevated temperature, decreasing Ti concentration to retard the formation of undesirable $\eta$ particles, and restricting silicon to discourage the G phase, as shown in Table 1. After solution annealing at 1149 °C (2100 °F) for 30 min, aging heat treatment at 760–800 °C for 4–16 h is recommended to enable Alloy 740/740H to form fine $\gamma'$-phase particles.

Alloy 282 was originally developed for gas turbine applications. Due to its excellent high-temperature creep strength, microstructural stability, and fabricability, Alloy 282 has also been found suitable for applications to A-USC power plants. After solution annealing at 1107–1149 °C (2025–2100 °F), a two-step aging heat treatment consisting of 1010 °C/2 h/air cool (AC) and 788 °C/8 h/AC is recommended to enable Alloy 282 to form fine $\gamma'$-phase particles [19].

### 3.2 Candidate Ni-base alloys in Europe

Figure 3 summarizes key Ni-base alloys in European A-USC projects. While Alloy 617 has been widely used in aircraft and land-based gas turbines, typically at temperatures above 800 °C, it is also one of the candidate Ni-base alloys for boiler and turbine components in A-USC power plants, because it offers a high resistance to both creep and oxidation. Precipitates of $\gamma'$ play an important role toward hardening inside the grains of Alloy 617 at around 700 °C, similar to the hardening process in Alloy 740 and Alloy 282. However, the precipitation hardening is much smaller in Alloy 617 than in Alloy 740 and Alloy 282, as can be seen from Figure 2 and Table 1. In the COMTES700 project, a test plant with large components made from Alloy 617B was implemented at the E.ON power plant at Scholven [3, 4]. Thus, it was demonstrated that the manufacture of such components was possible. The experience from the COMTES700 project was transferred to the follow-up projects, HWT II and ENCIO. The HWT II and ENCIO projects are intended to be the final step before the realization of the first 700 °C demonstration power plant.

### 3.3 Candidate Ni-base alloys in Japan

Table 3 gives the candidate Ni-base alloys for the main steam pipe and turbine rotor of A-USC projects in Japan [10]. In addition to conventional Ni-base alloys such as Alloy 263, Alloy 740, and Alloy 617, a variety of new Ni-base alloys were developed by materials and fabrication companies in Japan for application to A-USC power plants.

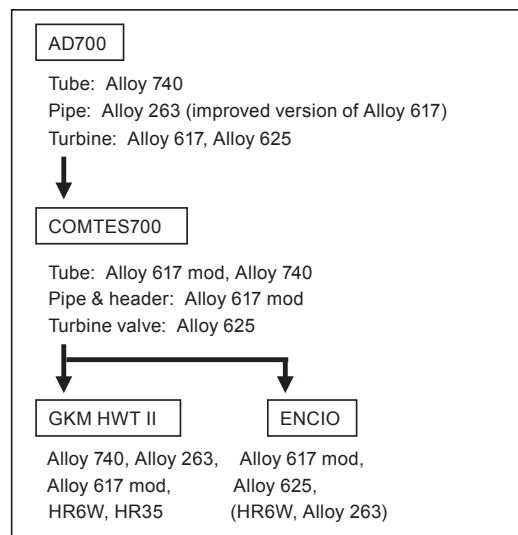HR6W was originally developed for SH tube applications.



Figure 3. Candidate Ni-base alloys in European A-USC projects.

Table 3. Candidate Ni-base alloys for thick section boiler and turbine components of A-USC project in Japan.

| Temperature | Component | Alloy | Chemical compositions |
|---|---|---|---|
| 700 °C | Main steam pipe | USC141* | Ni-20Cr-10Mo-1.2Al-1.6Ti |
| | | Alloy 263 | Ni-20Cr-20Co-6Mo-0.6Al-2.4Ti |
| | | Alloy 740 | Ni-25Cr-20Co-0.5Mo-0.9Al-1.8Ti-2Nb |
| | | Alloy 617 | Ni-22Cr-12Co-9Mo-1.2Al-0.3Ti |
| | | HR35* | 50Ni-30Cr-4W-Ti |
| | | HR6W* | Ni-23Cr-22Fe-7W |
| 700 °C | Turbine rotor | LTES700R* | Ni-12Cr-6Mo-7W-1.6Al-0.7Ti |
| | | FENIX700* | Ni-16Cr-36Fe-1.3Al-1.5Ti-2Nb |
| | | TOS1X-2* | Ni-18Cr-9Mo-12.5Co-1.25Al-1.35Ti-TaNb |

**Note:** *developed in Japan.

Due to its excellent creep and creep-fatigue properties and fabricability, HR6W has also been found suitable for application to thick section boiler components such as main steam pipes and headers in A-USC power plants [20, 21]. At first, HR6W was classified as austenitic steel, but is in fact a Ni-base alloy, because the concentration of Ni is higher than that of iron (Fe), although lower than Ni concentrations in conventional Ni-base alloys. The strengthening mechanisms of HR6W come from the combination of solid-solution hardening due to tungsten (W), and precipitation hardening due to fine $M_{23}C_6$ carbides, fine MX carbonitrides, and fine $Fe_2W$ Laves phase. This is quite different from the primary strengthening mechanism of most conventional Ni-base alloys, which is precipitation hardening due to fine $\gamma'$. The heat treatment of HR6W involves only solution annealing, with no aging heat treatment after solution annealing and prior to operation in power plants, which is also quite different from the treatment of conventional Ni-base alloys.

The new Ni-base alloys developed in Japan for A-USC power plants, such as LTES700R, USC141, FENIX700, and TOS1X-2, are modified versions of conventional Ni-base alloys [1]. Table 4 gives the alloy design philosophy for the modifica-

**Table 4. New Ni-base alloys developed in Japan for 700 °C A-USC power plants and alloy design philosophy for the modification of original Ni-base alloys.**

| New Ni-base alloy | Original alloy for modification | Alloy design philosophy for the modification of original Ni-base alloy |
|---|---|---|
| USC141 | Alloy 252 (Ni-9.7Mo-18Cr-10Co-1.1Al-2.7Ti) | Elimination of expensive Co, optimization of Al and Ti content for low thermal expansion and high strength |
| LTES700R | Refractaloy 26 (Fe-38Ni-18Cr-3Mo-0.2Al-2.6Ti-20Co) | Increase in Mo for low thermal expansion and high strength, increase in Al for $\gamma'$ strengthening |
| FENIX700 | Alloy 706 (Ni-36Fe-16Cr-3Nb-1.7Ti-0.3Al) | Decrease in Nb for minimum segregation and improved hot workability, increase in Al for $\gamma'$ strengthening |
| TOS1X-2 | Alloy 617 (Ni-22Cr-12Co-9Mo-1.2Al-0.3Ti) | Increase in Al and addition of Ta and Nb for $\gamma'$ strengthening |

tion of conventional Ni-base alloys. LTES700R (low thermal expansion superalloy for 700 °C) was alloy-designed to produce a new Ni-base alloy with a low thermal-expansion coefficient, similar to that of 12% Cr ferritic steel, and a high creep-rupture strength of 100 MPa or above at 700 °C and 100 000 h, similar to that of Refractaloy 26 [22, 23]. The alloy design philosophy for USC141 is the same as that of LTES700R: low thermal expansion and high creep-rupture strength [24]. FENIX700 (Fe-Ni-X superalloy for 700 °C) is a modified version of Alloy 706 with a higher creep-rupture strength of above 650 °C and a fewer solidification defects in large ingots [25]. FENIX700 is cheaper than the other Ni-base alloys, because of its higher content of Fe and hence lower Ni content. TOS1X-2 is a modified version of Alloy 617, made by increasing the Al concentration and adding tantalum (Ta) and niobium (Nb) for enhancing precipitation hardening due to $\gamma'$ [26]. The addition of Ta and Nb increases the amount of $\gamma'$ precipitate and retards the precipitation of the undesirable $\sigma$ phase.

## 3.4 Candidate Ni-base alloys in China and India

Figure 4 shows the candidate Ni-base alloys of the A-USC project in China, along with the ferritic and austenitic steels for pipes and tubes [12]. Alloy 617 and Alloy 740H are candidates for use in the highest temperature parts of pipes and tubes, respectively. Alloy 2984G is an upgraded version of a new Ni-Fe-base alloy, GH2984 (0.06C-19Cr-2Mo-1Nb-0.4Al-1Ti-33Fe-43Ni), which was developed by the Institute of Metal Research of the Chinese Academy of Sciences for application to tubes at temperatures above 650 °C.
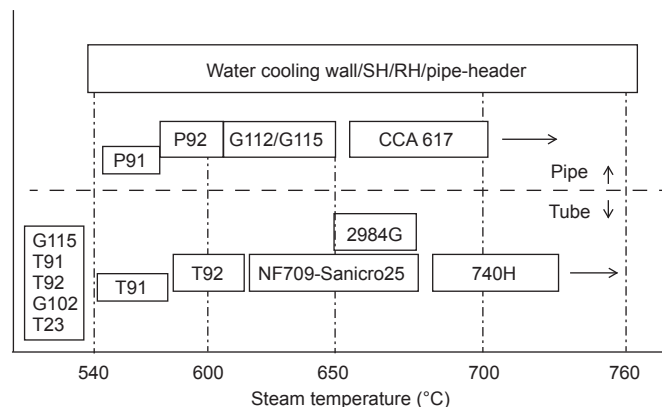


**Figure 4. Candidate ferritic and austenitic steels and Ni-base alloys for pipes and tubes of A-USC project in China.**

In India's National Mission for the Development of A-USC Technology, the materials selected for use in the high-

temperature zones of boilers for steam cycles at 710 °C/720 °C and 310 kg·cm$^{-2}$ are Alloy 617 mod and super 304H stainless steel [13]. Alloy 617 mod tubes were prepared by suitably modifying the chemical compositions within the ASME specification for Alloy 617. Turbine rotors would have an Alloy 617 mod forging for the high-temperature portion of a high pressure (HP)/intermediate pressure (IP) rotor, with dissimilar welded joints between cylindrical forgings of Alloy 617 mod and martensitic 10% Cr steel. The mission objectives include the development of advanced high-temperature materials, manufacturing technologies, and equipment design.

## 3.5 Mechanical properties and microstructure of candidate Ni-base alloys

### 3.5.1 Ni-base alloys strengthened by $\gamma'$ precipitates: Alloy 740/740H, Alloy 282, and Alloy 617

Figure 5 shows the creep-rupture data for Alloy 740 base metal and welded joints, as a function of the Larson-Miller parameter [27]. Various heats of Alloy 740 base metal, given in Table 5, with different chemistries and different grain sizes were subjected to creep-rupture testing. The materials of the base metal were given the standard aging heat treatment of 760–816 °C for 4–16 h after solution treatment, according to the ASME Code Case. Welded joints were prepared by gas tungsten arc welding (GTAW), gas metal arc welding (GMAW), and hot-wire narrow groove GTAW (hot-wire TIG). Table 6 provides the relevant welding details and postweld heat treatment given to the welded joints [27]. For the Alloy 740 base metal, the 100 000 h creep-rupture strength is evaluated to be 214.1 MPa, 123.7 MPa, and 84.8 MPa at 700 °C, 750 °C, and 800 °C, respectively, by the Larson-Miller parameter method with a constant $C$ value of 19.392, as shown in Figure 5(a). The lower scatter-band of creep-rupture data for the base metal is occupied by the heats with finer grain size, while slightly coarser grain size results in average or above average strength. Tortorelli et al. reported that little difference in creep-rupture results between Alloy 740 and Alloy 740H was found, although Alloy 740H showed significantly greater resistance to detrimental $\eta$-phase formation during creep-rupture testing [28].

In Figure 5(b), the creep-rupture data for welded joints with a variety of weld metals and heat-treatment conditions is located between the average strength line of the base metal, shown by the solid line, and the –30% strength line of the base metal, shown by the dotted line. The 30% reduction in stress is equivalent to a weld-strength factor (WSF) of 0.70. The 740GMAW and 740GTAW specimens exhibit a WSF slightly greater than 0.70, but the application of solution-
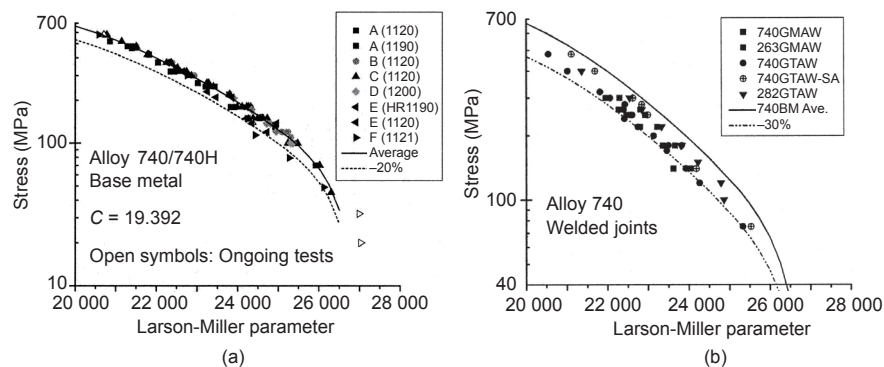
**Figure 5.** Creep-rupture data for Alloy 740 (a) base metal and (b) welded joints as a function of the Larson-Miller parameter.

annealing heat treatment after welding and prior to aging improves this to close to 0.90. The use of alternative filler metals, Alloy 263 and Alloy 282, also improves the WSF to 0.82 and 0.85, respectively.

For age-hardenable alloys such as Alloy 740, cold working is generally known to be detrimental to creep-rupture strength and creep-rupture ductility at elevated temperature [29, 30]. Figure 6 shows the ratio of the creep-rupture life of pre-strained Ni-base alloys to that of specimens without pre-strain, as a function of pre-strain [31]. The alloys were subjected to a pre-strain of 5%–15% at room temperature. Creep-rupture testing was carried out at 750 °C and at 225 MPa for Alloy 740/740H and Alloy 263, at 180 MPa for Alloy 617, at 100 MPa for HR6W, and at 160 MPa for HR35. Alloy 740/740H exhibits little or no effect from pre-strain for up to 5% pre-strain, while the ratio decreases to 0.5 or below for 7.5% pre-strain or more. Scanning electron microscope (SEM) observations after creep-rupture testing showed that grain boundaries (GBs) in the Alloy 740/740H specimens without pre-strain were almost entirely covered with precipitates of chromium (Cr) and Nb carbides. On the other hand, a number of precipitate-free zones were observed along GBs in pre-strained specimens of Alloy 740/740H, suggesting a reduction of GB precipitation hardening. Alloy 263 exhibits no effect of pre-strain on the creep

life at 750 °C for up to 15% pre-strain.

The fatigue data for Alloy 740H at 700 °C is shown in Figure 7, compared with the data for Alloy 617 and Alloy 263 [32]. Alloy 740H exhibits greater fatigue strength than Alloy 617 and Alloy 263, especially at low strain range. The fatigue limit of Alloy 740H is evaluated to be approximately half of the ultimate tensile strength.

The US DOE/OCDO A-USC project consortium has recognized that the tensile and fatigue behavior of Alloy 282 is adequate for application to a 760 °C rotor. The current HP and IP A-USC turbine design being considered calls for a bolted rotor, similar to an industrial gas turbine. In such a design, the highest temperature component is a forged disk. Trial ingots of Alloy 282 were produced via triple melting VIM/ESR/VAR, and were planned to be forged into a rotor disc for full property evaluation [19]. VIM, ESR, and VAR are acronyms for vacuum induction melting, electro slag re-melting, and vacuum arc re-melting, respectively. Because the two-step aging heat treatment after solution annealing for Alloy 282 would pose difficulties, especially for constructing large components in power plants, considerable efforts have been directed toward characterizing a one-

**Table 5.** Solution annealing temperature, grain size and chemical compositions of Alloy 740 base metal.

| Heat (SA temperature, °C) | Grain size (μm) | Composition (wt.%) (Ni balance) | | | | | | | | | | | | |
| --- | --- | --- | --- | --- | --- | --- | --- | --- | --- | --- | --- | --- | --- | --- |
| | | C | Mn | Fe | S | Si | Cr | Al | Ti | Co | Mo | Nb | P | B |
| **A (1120)** | 82.4 | 0.03 | 0.28 | 0.42 | 0.0010 | 0.54 | 24.43 | 0.94 | 1.81 | 20.00 | 0.55 | 1.98 | 0.005 | 0.0030 |
| **A (1190)** | 165 | | | | | | | | | | | | | |
| **B (1120)** | 188 | 0.03 | 0.26 | 0.46 | 0.0010 | 0.53 | 24.38 | 0.98 | 1.77 | 19.90 | 0.50 | 1.97 | 0.005 | 0.0043 |
| **C (1120)** | 127 | 0.03 | 0.26 | 0.46 | 0.0010 | 0.54 | 24.34 | 0.97 | 1.78 | 19.80 | 0.50 | 1.99 | 0.005 | 0.0037 |
| **D (1200)** | 169 | 0.03 | 0.27 | 1.02 | 0.0002 | 0.45 | 24.31 | 0.75 | 1.58 | 19.63 | 0.52 | 1.83 | 0.003 | 0.0006 |
| **E\* (1190)** | 89.6 | 0.06 | 0.30 | 0.69 | 0.0060 | 0.48 | 24.86 | 1.20 | 1.41 | 19.90 | 0.53 | 2.05 | 0.004 | 0.0010 |
| **E (1120)** | 113\*\* | | | | | | | | | | | | | |
| **F (1121)** | — | 0.04 | 0.31 | 1.05 | 0.0100 | 0.30 | 24.28 | 1.30 | 1.50 | 19.88 | 0.53 | 1.57 | 0.002 | 0.0007 |
| **G** | — | — | 0.30 | 1.07 | — | 0.20 | 24.35 | 1.28 | 1.45 | 20.08 | 0.53 | 1.53 | 0.002 | — |

**Notes:** \*material furnished in hot-rolled condition; \*\*bimodal grain size distribution, average grain size reported (center region grain size = 92.4 μm and outer sample region grain size = 145.1 μm); SA—solution annealed.

**Table 6.** Parameters for Alloy 740 welded joints.

| ID | Base metal | Product form | Welding process | Filler metal | Post-weld heat treatment |
| --- | --- | --- | --- | --- | --- |
| **740GMAW** | Alloy 740, heat B | 15.9 mm plate | GMA | Alloy 740 | 800 °C, 4 h |
| **263GMAW** | Alloy 740, heat B | 15.9 mm plate | GMA | Alloy 263 | 800 °C, 4 h |
| **740GTAW** | Alloy 740, heat A (1120 °C) | 50.8 mm OD, 10 mm WT tube | GMA | Alloy 740 | 800 °C, 4 h |
| **740GTAW-SA** | | | | | 1120 °C, 1 h AC |
| **282GTAW** | Alloy 740, heat G | 38.1 mm plate | Hot-wire TIG (GTA) | Alloy 282 | 800 °C, 4 h |

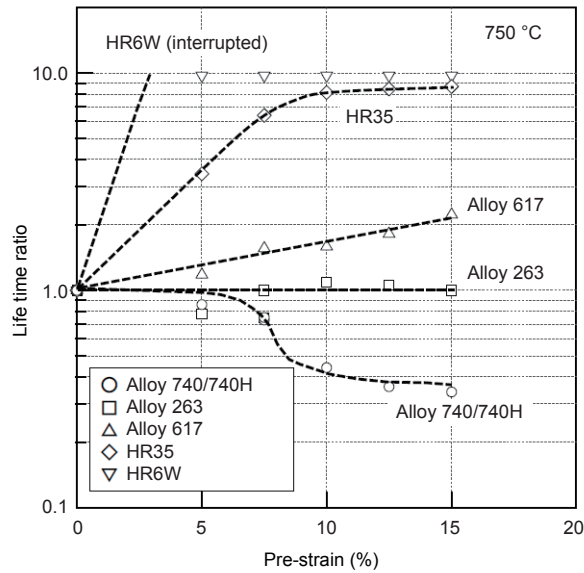**Notes:** OD—outer diameter; WT—wall thickness.

Figure 6. Effect of pre-strain on creep-rupture life of Ni-base alloys.
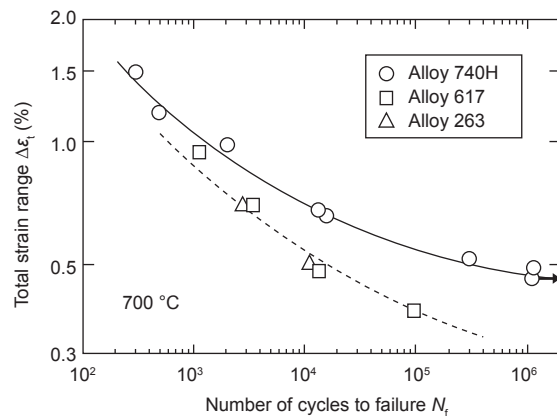


Figure 7. Total strain range for Alloy 740H, Alloy 617, and Alloy 263 at 700 °C versus the number of cycles to failure.

step aging heat treatment. Figure 8 shows the effect of different age-hardening treatments prior to creep-rupture testing on creep-rupture strength for Alloy 282, together with the data for Alloy 263 [19]. The creep-rupture testing was carried out over the temperature range of 649–816 °C (1200–1500 °F). The one-step aging heat treatment of 800 °C/8 h/AC results in a consistent, but very small, decrease in creep-rupture strength relative to the two-step aging heat treatment consisting of 1010 °C/2 h/AC plus 788 °C/8 h/AC. The decrease in creep-rupture strength is attributed to a slight coarsening of $\gamma'$-precipitate particles. The microstructure observations of Alloy 282 show that the two-step aging heat treatment leads to a discontinuous, blocky morphology of carbides (presumably $M_{23}C_6$) along GBs and fine distribution of $\gamma'$ particles having a size of 21–33 μm in the matrix. The one-step aging heat treatment causes a nearly continuous network of carbides along GBs, ledges protruding inside the grain, and $\gamma'$ particles having a size of 38–71 μm in the matrix. It is also noted that the creep-rupture strength of Alloy 282 is considerably higher than that of Alloy 263.

The European Creep Collaborative Committee (ECCC) Working Group 3C on Ni Alloys has performed assessments
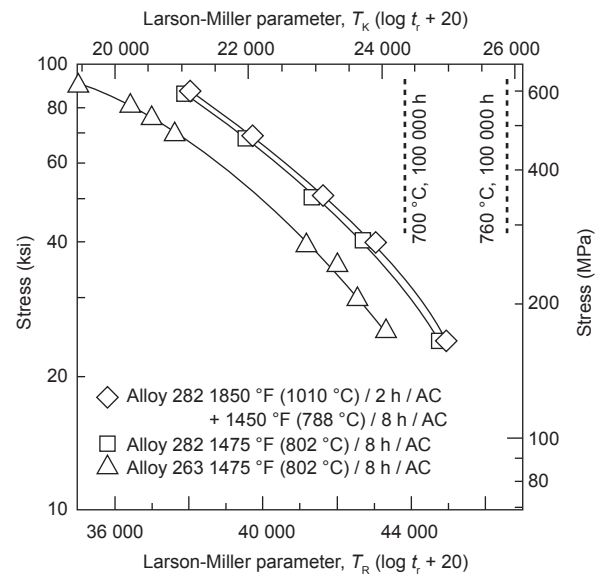


Figure 8. Creep-rupture data for Alloy 282 and Alloy 263 as a function of Larson-Miller parameter (**C = 20**). 1 ksi = 6.8947 MPa.

on a multi-heat creep-rupture data set for Alloy 617 at temperatures between 600 °C and above 1000 °C, using the data provided by Krupp, JRC Petten, and Special Metals [33]. A simple model with stress, log(stress), and $1/T$ terms (known by the acronym SLST) was chosen for the assessment. Figure 9 shows the creep-rupture data for Alloy 617 as a function of SLST parameter. The SLST model is given by

$$\ln (t_u^*) = -23.23283 - 0.018240476 \, \sigma_0 - 8.494174 \log(\sigma_0) + 52751.5156/T \tag{1}$$

where $t_u^*$ is the predicted rupture time in hours; $\sigma_0$ is the stress in MPa; and $T$ is the temperature in Kelvin [33]. The 100 000 h creep-rupture strength is assessed to be 179 MPa, 112 MPa, and 68 MPa at 650 °C, 700 °C, and 750 °C, respectively. However, the SLST model did not pass parts of the ECCC Post Assessment Tests, indicating that this model gave a poor fit to the creep-rupture data. This was partly due to the rather scattered creep-rupture data. The ECCC Working Group 3C reported that the only way to improve reliability in the rupture assessment for Alloy 617 would be to improve the extent of the creep-rupture data set, especially the extent of long-term data. Therefore, it was proposed that any future assessments of the creep-rupture strength of Alloy 617 should be based on an increased number of heats tested over a wide range of stresses and temperatures.

During the operation in COMTES700, some problems with thick-walled Alloy 617B components arose, such as the formation of cracks in a high-pressure bypass valve and in the HAZ of repair welds in a thick-walled steam pipe with a wall-thickness of 50 mm [4, 34]. Small cracks appeared along GBs in the HAZ of repair welds.

Three-point bending relaxation tests were carried out at 700 °C in order to understand the behavior of relaxation cracking in Alloy 617B components exposed to COMTES700. A virgin material of Alloy 617B that was subjected to solution annealing exhibited plastic deformation but no cracking during a three-point bending relaxation test, as shown in Figure
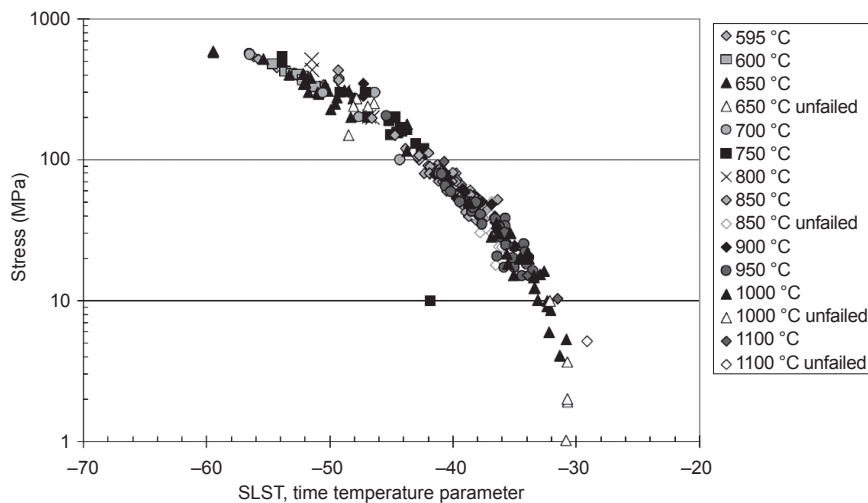
**Figure 9. Creep-rupture data for Alloy 617 as a function of SLST parameter.**

10(a) [4]. On the other hand, in the service-exposed Alloy 617B in COMTES700, after operation for three years at 700 °C, cracks formed during a three-point bending relaxation test, as shown in Figure 10(b) [4]. Microstructure observations show a series of Cr carbides mainly along GBs and a high density of fine $\gamma'$ precipitates inside the grains, causing significant hardening inside the grains by $\gamma'$ and loss of ductility. The $\gamma'$ precipitates can be re-dissolved by a heat treatment at 980 °C for 3 h. This heat treatment can reduce the susceptibility to relaxation cracking in Alloy 617B, resulting in no cracks in the base metal or in the repair welds of service-exposed Alloy 617B. However, thick welded joints without the heat treatment are broken during three-point bending relaxation tests at 700 °C.
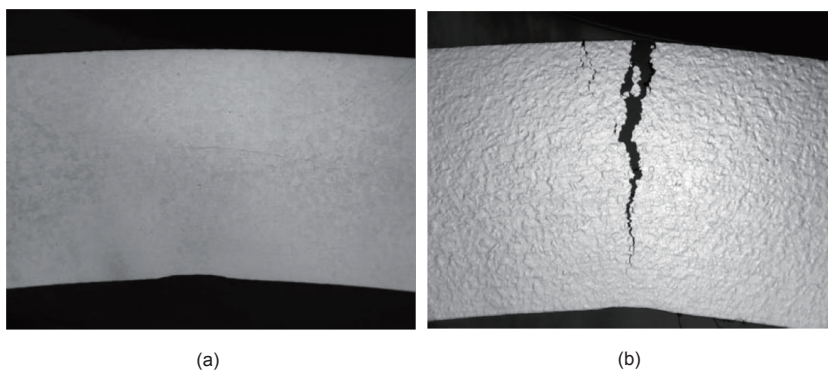


(a)                                         (b)

**Figure 10. (a) Solution-annealed and (b) service-exposed Alloy 617B specimens after three-point bending relaxation test.**

Recent results on the creep strength and microstructure of $\gamma'$-precipitation-hardened new Ni-base alloys developed in Japan, given in Table 3, are referred to in Ref. [35] for USC141, Ref. [36] for LTES700R, Ref. [37] for FENIX700, and Ref. [38] for TOS1X-2.

### 3.5.2 Ni-base alloy with no $\gamma'$: HR6W

Figure 11 shows the creep-rupture data for HR6W at 650–800 °C, indicating stable creep strength for up to long times [20, 21]. The 100 000 h creep-rupture strength is estimated to be 88 MPa, 64 MPa, and 46 MPa at 700 °C, 750 °C, and 800 °C, respectively, by the Larson-Miller parameter method. The creep-rupture strength is lower but the rupture elongation is larger in HR6W than in other Ni-base alloys strengthened by $\gamma'$, such as Alloy 617. Transmission electron microscope (TEM) observations show that the fine precipitates of $M_{23}C_6$, MX, and $Fe_2W$ Laves phase in HR6W

serve as an effective dislocation barrier.

The creep-fatigue properties of HR6W have been investigated at 700 °C, and compared with those of Alloy 617 [39]. Creep-fatigue tests were carried out under strain-controlled conditions at 700 °C, using fast-fast (PP) and slow-fast (CP) waveforms with strain rates of $0.8\%\cdot s^{-1}$ and $0.01\%\cdot s^{-1}$, respectively. The results are shown in Figure 12. Under the PP test condition, the fatigue life is almost the same for both HR6W and Alloy 617. However, the fatigue life of HR6W is much longer than that of Alloy 617 under the CP test condition, as a result of the greater creep-rupture ductility in HR6W than in Alloy 617. The SEM observations of fracture surface after the CP test show that intergranular cracking is dominant in Alloy 617 but that transgranular cracking is partly observed in HR6W. The intergranular cracking in Alloy 617 is attributed to the precipitation-hardening inside the grains by fine $\gamma'$ particles.

In order to investigate the susceptibility to relaxation cracking, slow strain-rate testing (SSRT) was carried out at a strain rate of $1 \times 10^{-6}$ s$^{-1}$ and at a temperature of 700 °C for HR6W, and compared with results for Alloy 617 [40]. HR6W maintains sufficient ductility in high strain-rate testing conditions, while Alloy 617 exhibits remarkable degradation in ductility. The results are correlated with intergranular cracking in Alloy 617, and with mainly transgranular cracking in HR6W.

With respect to the applicability of HR6W to A-USC power plants, the above results indicate that HR6W has advantages in creep-fatigue properties and resistance to relaxation cracking, while its creep-rupture strength is slightly lower than that of Alloy 617 at 700 °C.

## 4 New martensitic 9% Cr steels for low-temperature components of A-USC power plants

### 4.1 Candidate martensitic 9Cr steels

Figure 13 shows the development progress of martensitic boiler and turbine steels in Japan. The improvement of creep strength in martensitic 9%–12% Cr steels has been achieved by substituting
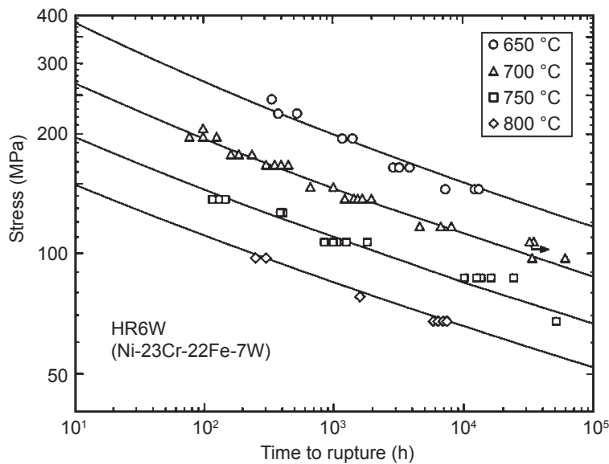
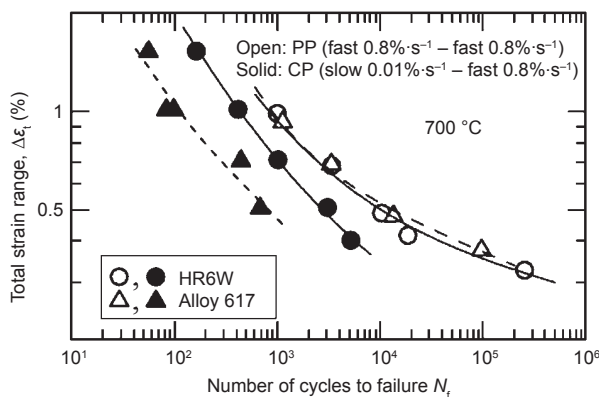**Figure 11. Creep-rupture data for HR6W at 650–800 °C.**



**Figure 12. Total strain range for HR6W and Alloy 617 at 700 °C versus the number of cycles to failure.**



**Figure 13. Development progress of martensitic boiler and turbine steels in Japan.** The steels in italic with asterisk were developed in Japan.

companies in Japan in the late 20th century before the start of the A-USC project, for application to turbine rotors with steam temperatures of 630 °C [45]. These rotor steels were originally intended to be used in 650 °C-class USC power plants. At present, however, Japan has no 650 °C-class USC power plant. Therefore, the rotor steels are ready for the construction of A-USC power plants. MTR10A, HR1200, and TOS110 are martensitic 10% to 11% Cr steels containing high W, Co, and B, which are upgraded versions of TMK2, HR1100, and TOS107, respectively.

In Europe, the development and evaluation of martensitic 9%–12% Cr steels for boilers and turbines of USC power plants has been continued within the frame of European Cooperation in Science and Technology (COST) programs: COST 501 (1986–1997), COST 522 (1998–2003), and COST 536 (2004–2009) [2, 46]. The target temperatures for the steels to be developed were set to be 600 °C, 620 °C, and 650 °C in the COST 501, COST 522, and COST 536 programs, respectively. The outcome of COST 522 was the demonstration of the manufacturability of large rotor forgings in an FB2 steel (9Cr-1Mo-1Co-0.2V-0.07Nb-0.01B-0.02N), the alloy with the highest potential for 620 °C application. In the COST 536 program, on the basis of the promising composition of FB2, the roles of Nb and Ta in long-term creep stability were investigated using a trial melt FB2-3Ta (8.9Cr-1.49Mo-1.0Co-0.2V-0.003Nb-0.013B-0.009N-0.08Ta) with higher silicon (Si) for steam oxidation resistance, a changed B/N ratio, the lowest Ni content, and the replacement of Nb with Ta [46]. The results of creep-rupture testing at 650 °C on a trial melt FB2-3Ta suggest that Ta in the chosen concentration would not be more effective than Nb in FB2.

Other strategies in Europe include the characterization of 9Cr steel with the same chemical composition as MARBN and the further optimization of MARBN, which are being conducted in several projects: the UK IMPACT project [47], the MACPLUS project [48], the Energy Materials Working Group (WG2), and EMEP (Engineered Micro- and Nanostructures for Enhanced Long-Term High-Temperature Materials Performance) [49, 50]. Their objectives are to develop ad-

part or all of the molybdenum (Mo) with W and also by the addition of cobalt (Co), nitrogen (N), Nb, and boron (B). The total concentration of alloying elements has been gradually increasing to improve the creep strength. An increase in the ferrite-forming element W requires higher Co, which is an austenite-stabilizing element, for the elimination of δ-ferrite. Three high-strength 9Cr steels, MARBN (9Cr-3W-3Co-VNbNB), Low-C 9Cr (9Cr-2.4W-1.8Co-VNb), and SAVE12AD (9Cr-2.9W-CoVNbTaNdN), are candidates for thick section boiler components such as main steam pipes operating at a maximum of 650 °C [10]. MARBN is a martensitic 9Cr steel strengthened by B and MX nitrides, which was alloy-designed on the basis of the stabilization of the martensitic microstructure in the vicinity of prior austenite grain boundaries (PAGBs) [41]. Low-C 9Cr was alloy-designed to stabilize the martensitic microstructure at elevated temperatures by minimizing Ni and Al impurities to be as low as possible [42]. The carbon concentration in this steel is reduced to 0.035%, which improves weldability. SAVE12AD contains high B but low N, and is similar to MARBN in this way [43]. The original SAVE12 contained a high Cr concentration of 12%, but in SAVE12AD the Cr concentration is reduced to 9% to achieve long-term stabilization of the martensitic microstructure [44].

MTR10A (10Cr-0.7Mo-1.8W-3Co-VNbB), HR1200 (11Cr-2.6W-3Co-NiVNbB), and TOS110 (10Cr-0.7Mo-1.8W-3Co-VNbB), as shown in Figure 13, were developed by fabrication
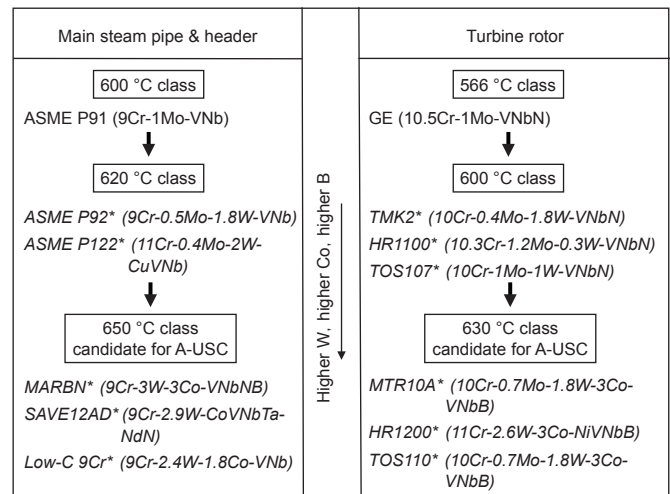
vanced MARBN to enable long-term safe operation at 650 °C.

G115, shown in Figure 4, is a martensitic 9Cr steel, which was developed in China for pipe applications at 650 °C or below and is now a candidate steel in the A-USC project in China [12, 51]. The chemical composition of G115 is 9Cr-3W-3Co-1CuVNbB steel containing 150 ppm B and 140 ppm N, which is similar to MARBN but for the addition of 1% copper (Cu).

### 4.2 Creep strength and microstructure of a new martensitic 9Cr steel: MARBN

Figure 14 shows the creep-rupture data for the base metal and welded joints of MARBN (containing 120–150 ppm of B and 60–90 ppm of N) at 650 °C, together with those for P92 and P122 [52, 53]. MARBN exhibits much higher creep-rupture strength of base metal than P92 and P122, as well as essentially no degradation in the creep-rupture strength of welded joints compared with the base metal, indicating no Type IV fracture. Dissimilar welded joints of MARBN/Alloy 617 and MARBN/Alloy 263 also exhibit substantially no degradation in creep-rupture strength compared with the MARBN base metal [54].
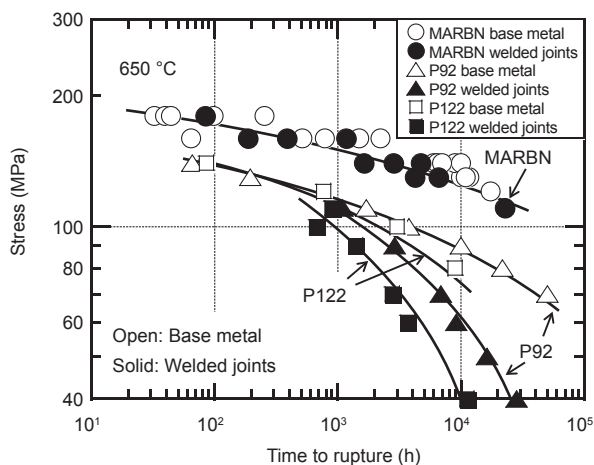


**Figure 14. Creep-rupture data for MARBN, P92 and P122 at 650 °C.**

The addition of B and N without the formation of any boron nitrides (BN) during normalizing heat treatment significantly improves the creep strength. However, excess addition of B and N causes the formation of BN during normalizing heat treatment; this formation consumes soluble B and N and hence degrades the creep strength. The formation of BN during normalizing heat treatment also degrades the creep-rupture ductility, as shown in Figure 15 [52, 53]. The addition of 300 ppm or 650 ppm of N together with 140 ppm of B significantly degrades the reduction of the area of 9Cr steel, because a large amount of BN formed during normalizing heat treatment in the steel. On the other hand, 9Cr steel containing less than 100 ppm of N exhibits an adequate reduction of area, larger than or the same as T91. This adequate reduction of area is advantageous to the creep-fatigue life, because the creep-fatigue life is proportional to the reduction of area in the creep-rupture testing; that is, it is proportional to the

creep ductility but not proportional to the creep strength. Gu et al. analyzed the creep voids formed in P92 steel after creep exposure [55]. Their analysis revealed that the majority of creep voids were associated with hard inclusions. Chemical analysis of these inclusions showed that the vast majority were BN, although some $Al_2O_3$ and MnS particles were also observed.
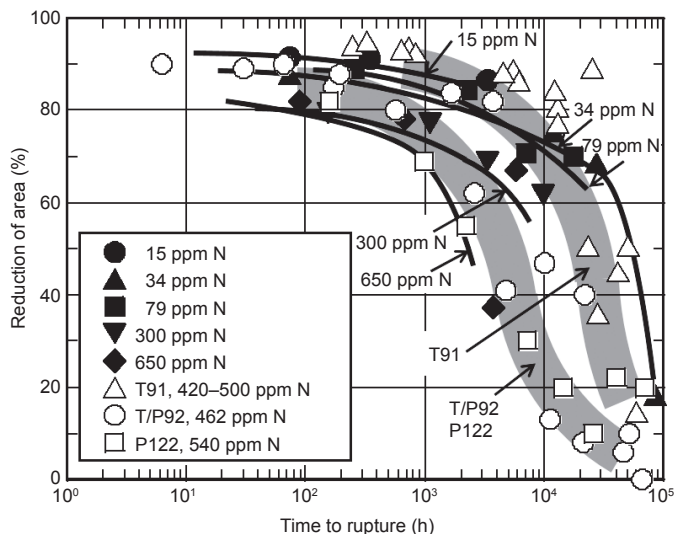


**Figure 15. Effect of N concentration on the reduction of area of 9Cr-3W-3Co-0.2V-0.05Nb steel containing 140 ppm B at 650 °C, together with data for T91, T/P92, and P122.**

The solubility product for BN in 9%–12% Cr steels at normalizing temperatures of 1050–1150 °C is given by

$$\log[\%B] = -2.45\log[\%N] - 6.81 \tag{2}$$

where [%B] and [%N] are the concentrations of soluble B and soluble N in mass fraction (%), respectively, as shown in Figure 16 [56]. At a B concentration of 140 ppm, only 95 ppm of N can dissolve in the matrix without the formation of any BN at a normalizing temperature.
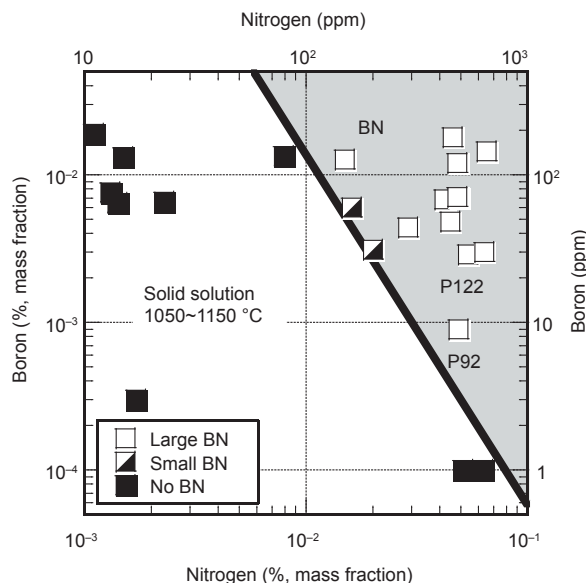


**Figure 16. Composition diagram of B and N for 9%–12% Cr steels at a normalizing temperature of 1050–1150 °C.**

The enrichment of soluble B near PAGBs by segregation is essential for the reduction in the coarsening rate of $M_{23}C_6$ carbides in the vicinity of PAGBs. This enrichment stabilizes the fine distribution of $M_{23}C_6$ carbides at and near PAGBs and enhances GB precipitation hardening for a long time [57].

In welded joints, the addition of B and N without any formation of BN during normalizing heat treatment causes no grain refinement and no Type IV fracture in the HAZ of MARBN. Diffusive $\alpha/\gamma$ transformation takes place in Gr. 92 during the heating of welding, while martensitic $\alpha/\gamma$ transformation takes place in the 9Cr-B steel. The diffusive transformation by the nucleation and growth of the $\gamma$ phase produces a fine-grained microstructure in the HAZ when the peak temperature is not too high. This fine-grained microstructure suggests the production of new GBs. Carbonitrides such as $M_{23}C_6$ also become dissolved during heating but cannot re-dissolve completely when the peak temperature is not too high. The resultant microstructure of Gr. 92 in the HAZ after post-weld heat treatment (PWHT) shows that very few precipitates are formed along PAGBs and essentially no lath-block substructure is formed. The production of new GBs and the incomplete dissolution of $M_{23}C_6$ carbides are responsible for the very few precipitates along GBs in the fine-grained microstructure. Very few $M_{23}C_6$ carbides along PAGBs suggest the reduction of GB-precipitation hardening. The degradation in creep strength of Gr. 92 welded joints is not caused by grain refinement in the HAZ but by the reduction of GB-precipitation hardening in the HAZ. On the other hand, the GB segregation of B retards the diffusive $\alpha/\gamma$ transformation during heating, because the GB segregation of B reduces GB energy and makes GBs less effective as heterogeneous nucleation sites for the $\gamma$ phase [57]. The resultant microstructure of the HAZ after PWHT is substantially the same as the original microstructure, with coarse grains and sufficient $M_{23}C_6$ carbides along GBs. Soluble B is essential for the change in transformation behavior during heating, resulting in no grain refinement and no Type IV fractures.

The formation of protective $Cr_2O_3$-rich scale is achieved on the surface of MARBN by pre-oxidation treatment in argon gas. This treatment significantly improves the oxidation resistance of MARBN in steam at 650 °C [58].

The creep strength and microstructure of the Chinese 9Cr steel G115 are reported by Liu et al. and Yan et al. [12, 51].

## 5 Summary

A variety of progress has been made in advancing materials technology on Ni-base alloys and martensitic 9%–12% Cr steels to enable A-USC power plants with maximum steam temperatures of 700 °C and above. The US DOE/OCDO A-USC project has led to extensive study on Alloy 740/740H and Alloy 282, which are strongly precipitation-hardened by a large amount of fine $\gamma'$ particles. The project consortium has identified Alloy 740/740H to be suitable for main steam pipes as well as for SH and RH tubes for long-term service in A-USC power plants with maximum steam temperatures of 760 °C, while Alloy 282 is promising for turbine rotors and discs. After exposure for three years at 700 °C in the COMTES700

project, thick-walled Alloy 617B components exhibited high susceptibility to relaxation cracking during a three-point bending relaxation test at 700 °C. The relaxation cracking is attributed to the precipitation hardening due to fine $\gamma'$ particles inside the grains. Post-exposure heat treatment at 980 °C for 3 h can re-dissolve $\gamma'$ precipitates, which results in no cracks in the base metal or in the repair welds of service-exposed Alloy 617B. In Japan, a variety of new Ni-base alloys were developed for application in A-USC power plants. HR6W with no $\gamma'$ has advantageous creep-fatigue properties and resistance to relaxation cracking, while its creep-rupture strength is slightly lower than that of Alloy 617 at 700 °C. New martensitic 9%–12% Cr steels, such as MARBN, Low-C 9Cr, SAVE12AD, and G115, were developed in Japan and in China for application to thick section boiler components at 650 °C and below. MARBN exhibits much higher creep-rupture strength of the base metal than P92 and P122, as well as essentially no degradation in creep-rupture strength of welded joints compared with base metal at 650 °C, indicating no Type IV fractures.

## 6 Future trends

Heat-resistant steels and alloys with higher microstructure stability exhibit higher long-term creep strength. GB embrittlement induced by impurity segregation and by the formation of harmful phases degrades creep-fatigue properties as well as the creep strength of Ni-base alloys. Extensive precipitation hardening inside the grains by a large amount of fine $\gamma'$ particles causes a mismatch of strength between GBs and inside the grains, which accelerates relaxation cracking and creep-fatigue cracking in Ni-base alloys. Therefore, more effort should be spent on examining Ni-base alloys in order to clarify the mechanisms of the microstructure evolution at and near GBs. It is also essential to establish a method to predict the evolution of GB microstructure at elevated temperatures using computational materials science and modern microstructure characterization techniques. Such efforts would contribute to the establishment of advanced Ni-base alloys with the best combination of microstructure at GBs and inside the grains.

Dissimilar welded joints between Ni-base alloys and martensitic 9%–12% Cr steels are inevitably present in both boiler and turbine components of A-USC power plants. Critical issues are the characterization of microstructure near fusion boundaries and in the HAZ, as well as the evaluation of long-term creep strength of dissimilar welded joints.

Reliable long-term creep-life prediction is another issue for both Ni-base alloys and martensitic 9%–12% Cr steels that needs to be investigated. Much attention should also be paid to incorporating research results on creep-deformation behavior and microstructure evolution in long-term creep while taking into account the predictions made by extrapolating short-term creep-rupture data. Such efforts would contribute to improvements in the reliability of new Ni-base alloys and new martensitic 9%–12% Cr steels for higher temperatures and longer service periods in A-USC power plants.

Finally, a scale-up of candidate Ni-base alloy ingots, the

manufacture of full-scale prototypes or model components, and subsequent component tests will be required prior to application to commercial plants. The effect of service exposure on mechanical properties should be investigated using specimens taken from the components. This testing contributes to the establishment of reliable methodologies to avoid unexpected damage in service-exposed materials, such as the relaxation cracking seen in Alloy 617 that had been exposed to the COMTES700 facility.

## References

1. F. Abe. Development of creep-resistant steels and alloys for use in power plants. In: A. Shirzadi, S. Jackson, eds. *Structural Alloys in Power Plants: Operational Challenges and High-Temperature Materials*. Cambridge, UK: Woodhead Publishing Limited, 2014: 250–293

2. R. Blum, R. W. Vanstone. Materials development for boilers and steam turbines operating at 700 °C. In: *Proceedings of the 6th International Charles Parsons Turbine Conference*. Dublin, Ireland, 2003: 498–510

3. H. Tschaffon. The European way to 700 °C coal fired power plant. In: *Proceedings of the 8th Liege Conference on Materials for Advanced Power Engineering 2006*. Liege, Belgium, 2006: 61–67

4. G. Gierschner, C. Ulrich, H. Tschaffon, F. Hansknecht. Latest developments for the flexible high efficient power plant of the future. In: *Proceedings of the 38th MPA Seminar*. Stuttgart, Germany, 2012: 353–373

5. K. Metzger, K. H. Czychon, K. Maile, A. Klenk, A. Helmrich, Q. Chen. GKM test rig: Investigation of the long term operation behavior of tubes and forgings made of alloys for future high efficient power plants. In: D. Gandy, J. Shingledecker, R. Viswanathan, eds. *Advances in Materials Technology for Fossil Power Plants: Proceedings from the Sixth International Conference*. Materials Park, OH: ASM International, 2013: 86–95

6. A. Di Gianfrancesco, A. Tizzanini, M. Jedamzik, C. Stolzenberger. ENCIO project: An European approach to 700 °C power plant. In: D. Gandy, J. Shingledecker, eds. *Advances in Materials Technology for Fossil Power Plants: Proceedings from the Seventh International Conference*. Materials Park, OH: ASM International, 2013: 9–23

7. R. Viswanathan, J. F. Henry, J. Tanzosh, G. Stanko, J. Shingledecker, B. Vitalis. U.S. program on materials technology for USC power plants. In: R. Viswanathan, D. Gandy, K. Coleman, eds. *Advances in Materials Technology for Fossil Power Plants: Proceedings from the Fourth International Conference*. Materials Park, OH: ASM International, 2005: 3–19

8. R. Viswanathan, J. Shingledecker, J. Hawk, S. Goodstein. Effect of creep in advanced materials for use in ultrasupercritical coal power plants. In: I. A. Shibli, S. R. Holdsworth, eds. *Creep & Fracture in High Temperature Components—Design & Life Assessment Issues: Proceedings of the 2nd ECCC Creep Conference*. Lancaster, PA: DEStech Publications, Inc., 2009: 31–43

9. J. Shingledecker, R. Purgert, P. Rawls. Current status of the U.S. DOE/OCDO A-USC materials technology research and development program. In: D. Gandy, J. Shingledecker, eds. *Advances in Materials Technology for Fossil Power Plants: Proceedings from the Seventh International Conference*. Materials Park, OH: ASM International, 2013: 41–52

10. M. Fukuda, et al. Advanced USC technology development in Japan. In: D. Gandy, J. Shingledecker, eds. *Advances in Materials Technology for Fossil Power Plants: Proceedings from the Seventh International Conference*. Materials Park, OH: ASM International, 2013: 24–40

11. R. Sun, Z. Cui, Y. Tao. Progress of China 700 °C USC development program. In: D. Gandy, J. Shingledecker, eds. *Advances in Materials Technology for Fossil Power Plants: Proceedings from the Seventh International Conference*.

12. Z. Liu, H. Bao, G. Yang, S. Xu, Q. Wang, Y. Yang. Material advancement used for 700 °C A-USC-PP in China. In: D. Gandy, J. Shingledecker, eds. *Advances in Materials Technology for Fossil Power Plants: Proceedings from the Seventh International Conference*. Materials Park, OH: ASM International, 2013: 171–179

13. A. Mathur, O. P. Bhutani, T. Jayakumar, D. K. Dubey, S. C. Chetal. India's national A-USC mission—Plan and progress. In: D. Gandy, J. Shingledecker, eds. *Advances in Materials Technology for Fossil Power Plants: Proceedings from the Seventh International Conference*. Materials Park, OH: ASM International, 2013: 53–59

14. F. Abe. Grade 91 heat-resistant martensitic steel. In: A. Shibli, ed. *Coal Power Plant Materials and Life Assessment: Developments and Applications*. Cambridge, UK: Woodhead Publishing Limited, 2014: 3–51

15. American Society of Mechanical Engineers. *ASME Boiler and Pressure Vessel Code, Section II—Materials, Part D—Properties (Metric)*. New York: The American Society of Mechanical Engineers, 2013

16. F. Abe. Stress to produce minimum creep rate of $10^{-5}$%/h and stress to cause rupture at $10^5$ h for ferritic and austenitic steels and superalloys. *Int. J. Pres. Ves. Pip.*, 2008, 85(1–2): 99–107

17. X. Xie, S. Zhao, J. Dong, G. D. Smith, B. A. Baker, S. L. Patel. A new improvement of Inconel Alloy 740 for USC power plants. In: R. Viswanathan, D. Gandy, K. Coleman, eds. *Advances in Materials Technology for Fossil Power Plants: Proceedings from the Fifth International Conference*. Materials Park, OH: ASM International, 2007: 220–230

18. S. Zhao, F. Lin, R. Fu, C. Chi, X. Xie. Microstructure evolution and precipitates stability in Inconel Alloy 740H during creep. In: D. Gandy, J. Shingledecker, eds. *Advances in Materials Technology for Fossil Power Plants: Proceedings from the Seventh International Conference*. Materials Park, OH: ASM International, 2013: 265–275

19. S. K. Srivastava, J. L. Caron, L. M. Pike. Recent developments in the characteristics of Haynes 282 alloy for use in A-USC applications. In: D. Gandy, J. Shingledecker, eds. *Advances in Materials Technology for Fossil Power Plants: Proceedings from the Seventh International Conference*. Materials Park, OH: ASM International, 2013: 120–130

20. M. Igarashi. Alloy design philosophy of creep-resistant steels. In: F. Abe, T. U. Kern, R. Viswanathan, eds. *Creep-Resistant Steels*. Cambridge, UK: Woodhead Publishing Limited, 2008: 539–572

21. H. Semba, H. Okada, M. Yonemura, M. Igarashi. Creep strength and microstructure in 23Cr-43Ni-7W alloy (HR6W) and Ni-base superalloys for advanced USC boilers. In: *Proceedings of the 34th MPA Seminar*. Stuttgart, Germany, 2008: 14.1–14.18

22. R. Yamamoto, et al. Development of Ni-based superalloy for advanced 700 °C-class steam turbines. In: R. Viswanathan, D. Gandy, K. Coleman, eds. *Advances in Materials Technology for Fossil Power Plants: Proceedings from the Fifth International Conference*. Materials Park, OH: ASM International, 2007: 434–446

23. R. Yamamoto, et al. Alloy design and material properties of Ni-based superalloy with low thermal expansion for steam turbine. *Tetsu-to-Hagane*, 2004, 90(1): 37–42

24. T. Ohno, et al. Development of low thermal expansion Ni base superalloy for steam turbine applications. In: R. Viswanathan, D. Gandy, K. Coleman, eds. *Advances in Materials Technology for Fossil Power Plants: Proceedings from the Fifth International Conference*. Materials Park, OH: ASM International, 2007: 377–390

25. S. Imano, J. Sato, K. Kajikawa, T. Takahashi. Mechanical properties and manufacturability of Ni-Fe base superalloy (FENIX-700) for A-USC steam turbine rotor large forgings. In: R. Viswanathan, D. Gandy, K. Coleman,

eds. *Advances in Materials Technology for Fossil Power Plants: Proceedings from the Fifth International Conference*. Materials Park, OH: ASM International, 2007: 424–433

26. S. Miyashita, M. Yamada, T. Suga, K. Imai, K. Nemoto, Y. Yoshioka. Development of a rotor alloy for advanced ultra super critical turbine power generation system. In: *Proceedings of the 34th MPA Seminar*. Stuttgart, Germany, 2008: 15.1–15.12

27. J. P. Shingledecker. Creep-rupture performance of Inconel Alloy 740 and welds. In: D. Gandy, J. Shingledecker, eds. *Advances in Materials Technology for Fossil Power Plants: Proceedings from the Seventh International Conference*. Materials Park, OH: ASM International, 2013: 230–241

28. P. F. Tortorelli, K. A. Unocic, H. Wang, M. L. Santella, J. P. Shingledecker. Creep-rupture behavior of precipitation-strengthened Ni-based alloys under advanced ultrasupercritical steam conditions. In: D. Gandy, J. Shingledecker, eds. *Advances in Materials Technology for Fossil Power Plants: Proceedings from the Seventh International Conference*. Materials Park, OH: ASM International, 2013: 131–142

29. J. P. Shingledecker, G. M. Pharr. Testing and analysis of full-scale creep-rupture experiments on Inconel Alloy 740 cold-formed tubing. *J. Mater. Eng. Perform.*, 2013, 22(2): 454–462

30. J. Shingledecker. Creep-rupture behavior of Ni-based alloy tube bends for A-USC boilers. In: *The Chinese Society for Metals (CSM) and the Minerals, Metals & Materials Society (TMS): Proceedings of Energy Materials 2014*. Xi'an, China, 2014: 161–168

31. K. Kubushiro, K. Nomura, H. Nakagawa. Effect of cold work on creep strength of nickel base alloys. In: J. Lecomte-Beckers, O. Dedry, J. Oakey, B. Kuhn, eds. *Proceedings of 10th Liege Conference on Materials for Advanced Power Engineering 2014*. Liege, Belgium, 2014: 754–756

32. S. Zhang, Y. Takahashi. Evaluation of high temperature strength of a Ni-base Alloy 740H for advanced ultra-supercritical power plant. In: D. Gandy, J. Shingledecker, eds. *Advances in Materials Technology for Fossil Power Plants: Proceedings from the Seventh International Conference*. Materials Park, OH: ASM International, 2013: 242–253

33. S. Chandra, R. Cotgrove, S. R. Holdsworth, M. Schwienheer, M. W. Spindler. Creep rupture data assessment of Alloy 617. In: *Proceedings of ECCC Creep Conference: Creep and Fracture in High Temperature Components—Design and Life Assessment Issues*. London, UK, 2005: 178–188

34. M. Speicher, A. Klenk, K. Maile, E. Roos. Investigations on advanced materials for 700 °C steam power plant components. In: *Proceedings of the 3rd Symposium on Heat Resistant Steels and Alloys for High Efficiency USC Power Plants 2009*. Tsukuba, Japan, 2009

35. T. Uehara, C. Aoki, T. Ohno, P. Schraven, H. Kamoshida, S. Imano. Creep rupture properties of Ni-base superalloy USC141 as solution treated for 700 °C class A-USC boiler. In: D. Gandy, J. Shingledecker, eds. *Advances in Materials Technology for Fossil Power Plants: Proceedings from the Seventh International Conference*. Materials Park, OH: ASM International, 2013: 1407–1416

36. R. Yamamoto, et al. Development and trial manufacturing of Ni-based superalloy "LTES700R" for advanced 700 °C class steam turbines. In: D. Gandy, J. Shingledecker, eds. *Advances in Materials Technology for Fossil Power Plants: Proceedings from the Seventh International Conference*. Materials Park, OH: ASM International, 2013: 468–481

37. K. Takasawa, T. Takahashi, R. Tanaka, T. Kure, S. Imano, E. Saito. Trial production and evaluation of 10-ton class A-USC turbine rotor of Ni-Fe base superalloy FENIX-700. In: D. Gandy, J. Shingledecker, eds. *Advances in Materials Technology for Fossil Power Plants: Proceedings from the Seventh International Conference*. Materials Park, OH: ASM International, 2013: 1283–1291

38. S. Miyashita, Y. Yoshioka, T. Kubo. Development and evaluation of large-scale rotor forging for over 700 °C-class A-USC steam turbine. In: D. Gandy, J. Shingledecker, eds. *Advances in Materials Technology for Fossil Power Plants: Proceedings from the Seventh International Conference*. Materials Park, OH: ASM International, 2013: 436–447

39. Y. Noguchi, M. Miyahara, H. Okada, M. Igarashi, K. Ogawa. Creep-fatigue properties of Fe-Ni base 0.08C-23Cr-45Ni-7W alloy for piping in 700 °C A-USC power plants. In: *Proceedings of the Eighth International Conference on Creep and Fatigue at Elevated Temperatures*. San Antonio, TX, USA, 2007: 261–266

40. H. Okada, T. Hamaguchi, H. Hirata, M. Yoshizawa. Development of HR6W and its applicability for thick-wall component for advanced USC boilers. In: *Proceedings of the 40th MPA Seminar*. Stuttgart, Germany, 2014: 137–146

41. F. Abe. Precipitate design for creep strengthening of 9% Cr tempered martensitic steel for ultra-supercritical power plant. *Sci. Technol. Adv. Mater.*, 2008, 9(1): 013002

42. T. Sato, K. Tamura, Y. Fukuda, K. Asakura, T. Fujita. Development of low-C 9Cr steel for USC boilers. *CAMP-ISIJ*, 2006, 19: 565 (in Japanese)

43. K. Metzger, K. H. Czychon, E. Roos, K. Maile. Testing for the investigation of the damage mechanism of high-temperature for the 700 °C power plant. In: *Proceedings of the 34th MPA Seminar*. Stuttgart, Germany, 2008: 48.1-48.12

44. M. Igarashi, Y. Sawaragi. Development of 0.1C-11Cr-3W-3Co-V-Nb-Ta-Nd-N ferritic steel for USC boilers. In: *Proceedings of International Conference on Power Engineering-97 (ICOPE-97)*. Tokyo, Japan, 1997: 107–112

45. K. H. Mayer, F. Masuyama. The development of creep-resistant steels. In: F. Abe, T. U. Kern, R. Viswanathan, eds. *Creep-Resistant Steels*. Cambridge, UK: Woodhead Publishing Limited, 2008: 15–77

46. T. U. Kern, K. H. Mayer, B. Donth, G. Zeiler, A. Di Gianfrancesco. The European efforts in development of new high temperature rotor materials COST536. In: J. Lecomte-Beckers, Q. Contrepois, T. Beck, B. Kuhn, eds. *Proceedings of 9th Liege Conference on Materials for Advanced Power Engineering 2010*. Liege, Belgium, 2010: 27–36

47. P. Barnard, et al. A new MarBN alloy for USC power plant. In: *Proceedings of 5th Symposium on Heat Resistant Steels and Alloys for High Efficiency USC/A-USC Power Plants 2013*. Seoul, Korea, 2013: 31

48. E. Zanin, et al. Component performance-driven solutions for long-term efficiency increase in ultra supercritical power plants Macplus Project. In: J. Lecomte-Beckers, O. Dedry, J. Oakey, B. Kuhn, eds. *Proceedings of 10th Liege Conference on Materials for Advanced Power Engineering 2014*. Liege, Belgium, 2014: 803–819

49. C. Sommitsch, et al. Co-ordination of European research in structural materials for power generation equipment. In: J. Lecomte-Beckers, O. Dedry, J. Oakey, B. Kuhn, eds. *Proceedings of 10th Liege Conference on Materials for Advanced Power Engineering 2014*. Liege, Belgium, 2014: 3–18

50. E. Plesiutschunig, C. Beal, S. Paul, G. Zeiler, S. Mitsche, C. Sommitsch. Microstructure for an optimized creep rupture strength of high Cr steels. In: J. Lecomte-Beckers, O. Dedry, J. Oakey, B. Kuhn, eds. *Proceedings of 10th Liege Conference on Materials for Advanced Power Engineering 2014*. Liege, Belgium, 2014: 180–188

51. P. Yan, Z. Liu, Y. Weng. Effect of preferential heat treatment on microstructure of new martensitic heat resistant steel G115. In: *The Chinese Society for Metals (CSM) and the Minerals, Metals & Materials Society (TMS): Proceedings of Energy Materials 2014*. Xi'an, China, 2014: 137–144

52. F. Abe. Effect of boron on long-term stability of 9Cr steel for 650 °C boilers. In: *Proceedings of the 38th MPA Seminar*. Stuttgart, Germany, 2012: 305–314

53. F. Abe, M. Tabuchi, S. Tsukamoto. Alloy design of martensitic 9Cr-Boron steel for A-USC boiler at 650 °C—Beyond Grades 91, 92 and 122. In: *The*

Chinese Society for Metals (CSM) and the Minerals, Metals & Materials Society (TMS): Proceedings of Energy Materials 2014. Xi'an, China, 2014: 129–136

54. M. Tabuchi, H. Hongo, F. Abe. Creep strength of dissimilar welded joints using high B-9Cr steel for advanced USC boiler. *Metall. Mater. Trans. A*, 2014, 45(11): 5068–5075

55. Y. Gu, G. D. West, R. C. Thomson, J. Parker. Investigation of creep damage and cavitation mechanisms in P92 steels. In: D. Gandy, J. Shingledecker, eds. *Advances in Materials Technology for Fossil Power Plants: Proceedings from the Seventh International Conference*. Materials Park, OH: ASM International, 2013: 596–606

56. K. Sakuraya, H. Okada, F. Abe. BN type inclusions formed in high Cr ferritic heat resistant steel. *Energy Materials*, 2006, 1(3): 158–166

57. F. Abe, M. Tabuchi, S. Tsukamoto. Mechanisms for Boron effect on microstructure and creep strength of ferritic power plant steels. *Energy Materials*, 2009, 4(4): 166–174

58. H. Okubo, S. Muneki, T. Hara, H. Kutsumi, F. Abe. Improvement of oxidation resistance of 9% Cr steel for A-USC by pre-oxidation treatment. In: *Proceedings of the 34th MPA Seminar*. Stuttgart, Germany, 2008: 42.1–42.11